Green and simple approach for low-cost bioproducts preparation and CO_2 capture

Gabriela Durán-Jiménez[*1], Emily T. Kostas[2], Lee A. Stevens[1], Will Meredith[1], Maria Erans[1], Virginia Hernández-Montoya[3,] Adam Buttress[1], Clement N. Uguna[1], Eleanor Binner[1]

[1]Faculty of Engineering, the University of Nottingham, University Park, Nottingham, NG7 2RD, U.K

[2] Department of Biochemical Engineering, University College London, Gower Street, London, WC1H 6BT, UK.

[3]TecNM/Instituto Tecnológico de Aguascalientes, Av. Adolfo López Mateos No. 1801 Ote. C.P. 20256, Aguascalientes, México.

* Corresponding author

e-mail: Gabriela.duranjimenez1@nottingham.ac.uk

Tel: +44 (0)77 2793 4248

Abstract

This study has demonstrated, for the first time, a simple, fast and flexible microwave processing method for the simultaneous preparation of bio-products (bio-oil, bio-gas and biochar) using a methodology that avoids any form of catalyst or chemical activation. The dielectric properties of biomass and physicochemical characterisation such as TGA, elemental and proximate analysis, XRD, SEM/EDX and textural properties, showed that 8 kJ g^{-1} of microwave energy can produce superior biochars for applications in CO_2 capture. The maximum CO_2 uptake capacity for biochar produced was 2.5 mmol g^{-1} and 2.0 mmol g^{-1} at 0 and 25 °C and 1 bar, which and also exhibited high gas selectivity compared with N_2, fast kinetics of adsorption (<10 min) and desirable reusability (>95 %) after 20 cycles. GC-MS analysis of generated bio-oil products revealed that higher microwave energies (>8 kJ g^{-1}) significantly enhanced the amount of bio-oil produced (39 %) and specifically the formation of levoglucosan, furfural and phenolics compounds, and bio-gas analysis identified trace levels of H_2 and CH_4. The results from this study confirm a green, inexpensive and efficient approach for biomass valorisation which can easily be embedded within bio-refinery process, and also demonstrates the potential of biochars for post-combustion CO_2 uptake.

KEYWORDS: Lignocellulosic Biomass, Microwave pyrolysis, Bio-oil, Biochar, CO_2 capture

1 Introduction

The issues regarding climate change have attracted considerable attention, particularly since the average global temperature has been estimated to increase due to the greenhouse gas emissions. In 2011, the European Union reaffirmed its objective to reduce carbon dioxide (CO_2) emissions by 80-90 % ("Nations, U. Paris Agreement to the United Nations Framework Convention on Climate Change," 2015)(Zappa et al., 2019). In order to achieve these goals, research efforts have focussed on the sustainable valorisation of biomass feedstocks and their conversion into energy, fuels and bio-products; with emphasis on processes that can reduce emissions and promotes circular bio-economy (Acevedo-García et al., 2020)(Olabi, 2019).

The transformation of biomass residues to chemicals has the potential to produce bio-products base for bio-refinery, adhesives, surfactants and plasticisers using technologies such as fermentation, extraction, hydrolysis, gasification and pyrolysis. In this sense, it is estimated that more than 422,800 tons of pecan nut shell (NS) (*Carya illinoinensis*) are produced yearly, representing a significant volume of waste available for the generation of added value bio-products (Agustin-Salazar et al., 2018). Recent reports highlight its use for the preparation of reduced sugars (Santos et al., 2020), as reinforcing filler in poly (lactic acid) biocomposites (Agustin-Salazar et al., 2018), gasification for syngas generation (Aldana et al., 2015) (Lozano and Lozano, 2018) and as precursor of adsorbent for energy storage (Martínez-Casillas et al., 2019).

Amongst the available thermochemical processes, microwave pyrolysis has proved to be a very attractive processing technology, due to its nature and volumetric heating which offers the possibility to heat selectively and therefore maximize the production of desired products (Durán-Jiménez et al., 2015)(Kostas et al., 2020)(Kostas et al., 2017)(Beneroso et al., 2017). The heating effect resulting from the interaction of microwave energy with biomass

predominantly occurs through coupling of both permanent and induced dipoles, as well as ionic components of the material to the oscillating electromagnetic field. This motion then induces molecular friction and generation of heat within the volume of the material (Kostas et al., 2019). The energy is transferred from inside to outside of the particle which results in an inverted temperature gradient (Haeldermans et al., 2019)(Kostas et al., 2017). Compared with conventional heating, this technology offers a variety of advantages, such as greener instantaneous heating and the elimination of catalyst or other auxiliary chemicals, which means that wastes are not generated (Durán-Jiménez et al., 2020)(Yin, 2012). By the evaluation of dielectric properties, microwave have proved to be compatible with biomass feedstock pyrolysis processes to generate a range of bio-based products including bio-oils and biochars (Kostas et al., 2019)(Yin, 2012)(J. Li et al., 2016)(Kostas et al., 2020)(Sears et al., 2006)(Durán-Jiménez et al., 2016)(Ferrera-Lorenzo et al., 2014). Bio-oils typically contain a mixture of oxygenated compounds (Kan et al., 2016), and have the potential to be catalytically upgraded to fuel. Biochar is a porous carbon-based material used in several applications including batteries, catalyst, soil remediation and as adsorbent of pollutants in liquid and gas systems (Li et al., 2017)(Kan et al., 2016).

Nowadays, several materials such as fly ashes (Bui Viet et al., 2020) biomass, cement kiln dust, paper sludge, sewage sludge (Sanna et al., 2012), activated carbons (Srinivas et al., 2014)(Hoseinzadeh Hesas et al., 2015)(Yang et al., 2017), zeolites and metal organic frameworks (Lin et al., 2014)(Liang et al., 2009)(Saha et al., 2010) have been investigated for CO_2 capture. Particular interest in the preparation of biochar for CO_2 capture has also been reported due to its simplicity and low cost (Huang et al., 2015). However, research has focused on the modification of biochar by chemical and physical activation (Li and Xiao, 2019)(Y. Li et al., 2016)(C. Zhang et al., 2016) or the incorporation of metals into the skeleton of biochars (Lahijani et al., 2018) to enhance their CO_2 adsorption capacity. This modification has resulted

in the increase of the costs and difficulties in the regeneration limiting its industrial application.

Currently, there is a huge need in the study of more environmentally friendly processes for the synthesis of biochars with effective adsorption properties. However, the global biomass valorisation (liquid, solid and gas fraction) and the detailed assessment of CO_2 adsorption capacities of biochars obtained without chemical modification and microwave heating, have not been evaluated. The conversion of waste biomass feedstocks into added-value products will address issues related to its disposal, which is essential for a sustainable global circular bio-economy (Acevedo-García et al., 2020). Furthermore, the application of products generated in one step that also avoids the use of catalysts is highly appealing from an environmental and energy consumption perspective.

To our knowledge, this is the first study that employs nut shell as a renewable source that complies within a bio-refinery setting for multiple generation of added value products. This study does not only focus on the characterisation of generated bio-oil from microwave pyrolysis process, but also in the application of biochar. A detailed discussion of the physicochemical characterisation and evaluation of the simple-to-produce biochars for post-combustion CO_2 capture is presented, with assessments focussing on the kinetics, selectivity, reusability and equilibrium of adsorption of CO_2 at relevant temperatures (0 and 25 °C).

2 Materials and methods

2.1 Materials

In this study pecan nut shell (NS) was used as raw material. Prior to pyrolysis experiments, NS was washed and dried at 70 °C.

2.2 Biomass pyrolysis experiments

The system used in the microwave pyrolysis is shown in Fig. 1, and is composed by one mode

applicator, 2 kW microwave generator (2.45 GHz), an automatic tuner (S-TEAM STHD v1.5) and sliding short to maximise the power density in the sample. (Durán-Jiménez et al., 2020). The sample was placed in a quartz reactor in nitrogen atmosphere (2 L min^{-1}).

The microwave processing conditions were in the range of 300-400 W input power and 2 to 6 min duration time as shown in Table S1. The liquid fraction was stored in a pre-weighed vials at 4 °C. The non-condensable gases were passed into a gas line and collected using a tedlar gas bag for subsequent analysis.

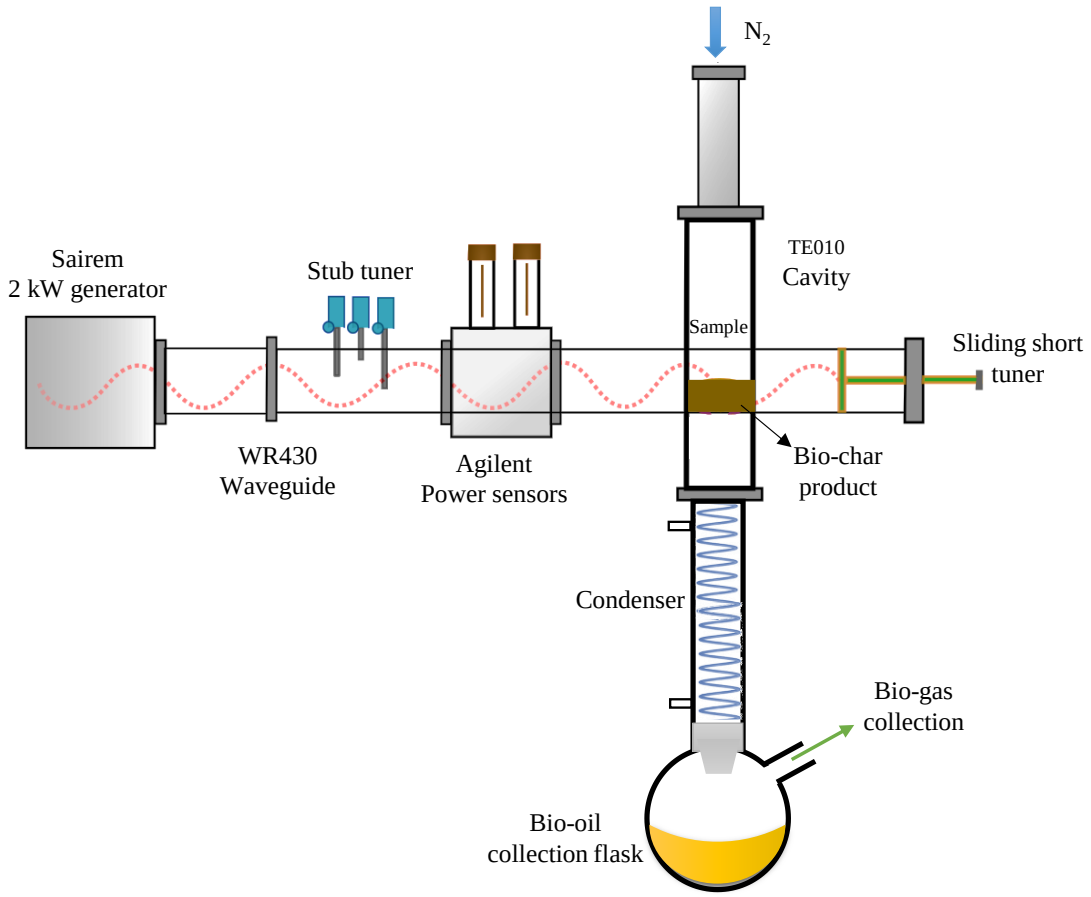

Fig. 1. Microwave pyrolysis system used in this work

It should be noted that it is unfeasible to accurately measure the sample temperature as microwave heating causes volumetric and instantaneous heating (Nagahata and Takeuchi, 2019).

The biochar and bio oil yield were quantified by their weights and the yield of the non-condensable product was calculated by difference as follow:

$$Y_{Bio-char} = \frac{M_{Bio-char}}{M_0} \times 100 \quad (1)$$

$$Y_{Bio-oil} = \frac{M_{Bio-oil}}{M_0} \times 100 \quad (2)$$

$$Y_{Bio-gas} = 100 - [Y_{Bio-char} + Y_{Bio-oil}] \quad (3)$$

2.3 Characterisation techniques

2.3.1 Dielectric properties

The dielectric response of a material is commonly presented as permittivity (ε) which can be given by:

$$\varepsilon = \varepsilon_0 \varepsilon_r = (\varepsilon_r' - j\varepsilon_r'') \quad (4)$$

where ε_0 is permittivity of the free space (8.854x10-12 F m^{-1}), ε_r is complex relative permittivity, and j is imaginary unit (j^2=-1). The complex relative permittivity is composed by the real part, called relative dielectric constant (ε_r'), and it is a measure of the ability of the material to store electrical energy; and the imaginary part, (ε_r'') known as relative dielectric loss factor, represents the energy dissipated. Dielectric properties of NS were obtained using the cavity perturbation technique for a temperature range of 20 - 650 °C at 2450 MHz (Durán-Jiménez et al., 2020). The sample was placed in the system using a quartz tube of (ID) 3 mm that is moved by an automated motor to the furnace and cylindrical TM0n0 mode cavity. The dielectric properties were calculated using the cavity response between a load and empty tube measured by a HP 8753 vector network analyzer (VNA). The results presented in this work are the averages of 3 replications.

2.3.2 Bio-gas and Bio-oil Analysis

The bio-gas generated during the pyrolysis experiments were analysed as described somewhere else (Almustapha et al., 2017), using a Clarus 580 Gas Chromatograph (GC) system.

The bio-oil were analysed by GC-MS using a Varian CP-3800 GC incorporated to a Varian 1200 MS (70 eV, EI mode) (Kostas et al., 2019). The identification of the compounds in the bio-oils was determined according to the NIST Mass Spectral library from the National Institute of Standards and Technology, Maryland, USA.

2.3.3 Biochar and NS characterisation

Proximate analysis was conducted by the method previously described by Donahue (Donahue and Rais, 2009). The sample was placed in TGA Q500 TA Instrument and heated to 900 °C under a N_2 atmosphere (100 ml min^{-1}, 1 bar) and then held at 900 °C for 15 min, the atmosphere was then switched to air and held for a further 15 min. The ultimate analysis was determined using a LECO CHN-628 elemental analyzer. A Philips XL 30 microscope was used to analyze the morphology and the X-ray diffractograms were obtained by using a Bruker D8 Advance Da Vinci.

The textural parameters were calculated from the N_2 adsorption isotherms at -196 °C using a Micromeritics ASAP 2420 apparatus. Brunauer–Emmett–Teller (BET) theory was used to calculate the surface area while the micropore, total pore volume and size distributions were determined by Non-Local Density Functional Theory (NLDFT) (Thommes et al., 2015) (Adeniran et al., 2014) by combining a CO_2 adsorption isotherm at 0 °C to a N_2 adsorption isotherm.

2.4 CO_2 capture experiments

The CO_2 uptake of the generated biochars were determined by thermogravimetric and volumetric analysis. The volumetric experiments were conducted in a Micromeritics ASAP 2420 analyser, where approximately 500 mg of biochar was degassed at 120 °C in N_2 for 15 h. The amount of CO_2 adsorbed was determined using 100 % CO_2 in the range of 0.001 to 1.2 bar. The thermogravimetric uptake was performed using a TGA Q500 TA instrument.

Approximately 25 mg of biochar was placed in a pan and dried for 30 min at 120 °C and atmospheric pressure. After the physiosorbed moisture was removed, the sample was cooled down to 25 °C and the gas was switched at 100% CO_2. Once the adsorption reached equilibrium, the adsorbed amount of CO_2 was recorded vs time for 60 min, then the sample was heated up to 120 °C in N_2 for 15 min to complete the CO_2 desorption. In total, 20 adsorption-desorption cycles were conducted to determine stability and recyclability of the biochar. The selectivity was determined by thermogravimetric analysis at 25 °C using N_2 (100 ml min^{-1}) for the adsorption stage and Ar in the desorption stage. All experiments were performed in triplicate and the averages are presented. In general, standard deviations were below 5 % of average values.

3 Results and Discussion

3.1 Microwave pyrolysis and bio-product formation mechanism

The TG and DTG curves obtained from the pecan NS and the dielectric characterisation are shown in Fig. 2. Based on the thermograms, the decomposition of the biomass occurs in three main stages. The first stage involves the removal of water at temperatures up to 150 °C, whereas the second and third stages describe the hemicellulose and cellulose decomposition (up to 400 ° C), and the lignin transformation into char (beyond 400 °C).

In microwave heating, the dielectric constant and loss factor determine the capability of the biomass to be heated by microwave heating. The results of dielectric characterisation illustrate that at temperatures below 150 °C, is the water the main responsible for the microwave absorption due to dipolar mechanisms. When the water is removed the dipolar movements decreased leading to the reduction the dielectric constant and loss factor. However, at temperatures above 600 °C the formation of char is promoted and hence an exponential increase in the dielectric properties is observed, as results of the increase in the conductivity of

the sample. Similar behaviour for lignocellulosic biomasses have been previously reported (Miura et al., 2004)(Namazi et al., 2015).

The distribution of the three pyrogenic products generated from the pyrolysis of NS using microwave heating, are presented in Table S1. The yields of biochar are in the range of 16 – 18 %. It has been reported the bio-oil yields for lignocellulosic biomasses such as pine wood and corn stover ranges between 20- 40 % (Kan et al., 2016) (Jung et al., 2019). Similar yields were found in this study (21.5 - 40 %).

The results indicate the higher bio-oil yields are a result of the faster processing times achieved in microwaves, and also confirm that microwave pyrolysis could be thermochemically faster than slow pyrolysis in a conventionally heated process (Huang et al., 2015). The bio-oil yields were correlated to the specific energy, which is a measure of the real absorbed energy by the sample under processing. It appeared that at higher energies but low intensities (300 W) is possible to obtain higher bio-oil yields, which can be as result of a more controlled volatile matter evolution in the pyrolysis process. For example, the samples prepared at 300 W showed a positive trend where the highest bio-oil yield (39.0%) corresponds to the higher specific energy (8 kJ g^{-1}). This behaviour, was different for bio-oils produced using incident power of 400 W where the yield decreased for samples prepared at higher energy (24.8% at 8.4 kJ g^{-1}) This phenomena can be explained in terms of heating rate and power density. For samples IV-N (300 W - 6 min) and VII-NS (400 W – 4 min), similar specific energy was reported, however in VII-NS the heating rate and power density were higher, leading to the preferred gas production and lower bio-oil yields.

This study confirms that the NS bio-oil yield is highly governed for the energy, but also for the power density used in the pyrolysis. This is of great relevance and establish the basis for microwave processing where the maximisation of bio-oil is priority.

The complex transformation of biomass into biochar and bio-oil has been proposed as result of several depolymerisation reactions. The model describes groups in cellulose and hemicellulose such as glucomannans and containing glycosidic bond that broke down to into levoglucosan that further undergoes dehydration and intramolecular arrays to produce furfural and furan (Singh et al., 2019). Lignin is a complex cross- linked polysaccharide and its decomposition results in the formation of the biochar network (J. Li et al., 2016). The polymerisation and aromatisation mechanisms produce the formation of wide-range phenols in the liquid phase and rich carbon content solid (biochar).

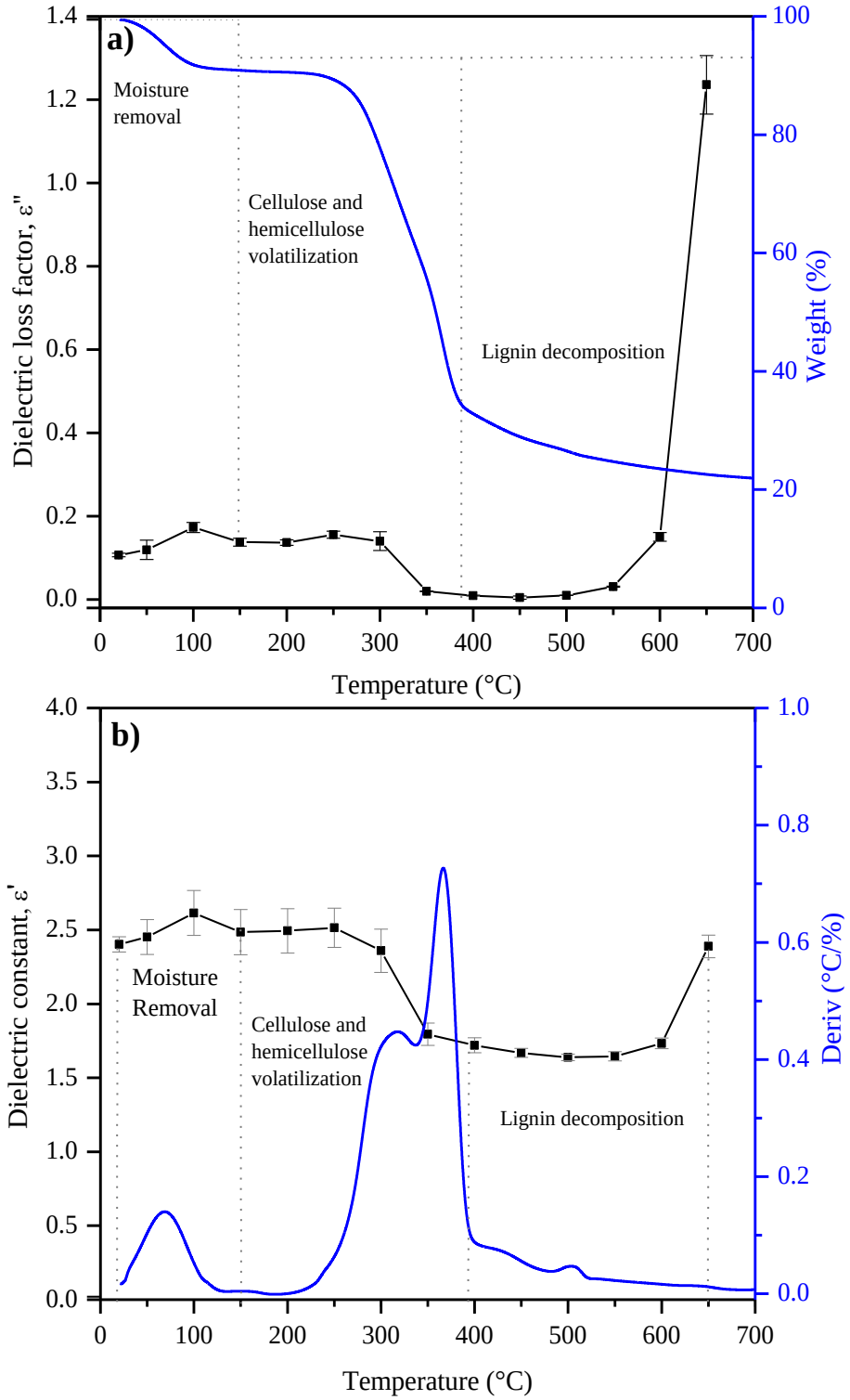

Fig. 2. Dielectric properties and TGA (a) & DTG (b) pecan NS as a function of temperature

3.2 Bio-oil and bio-gas characterisation

The most prominent compounds identified in bio-oils were semi-quantitatively analysed and

are shown in Table 1. Fig. 3 illustrates a typical GC-MS total ion chromatogram, and all samples are shown in Fig. S1. It can be seen that bio-oils are a mixture of numerous organic compounds that have resulted from the pyrolytic breakdown of lignin, cellulose and hemicellulose as per in Fig. S2, which include water, vanillins, furan carboxaldehydes, pyrones, acetic acid, hydroxy-aldehydes and phenolics. A range of phenolic based compounds such as methoxyphenol, dimethylphenol, ethylmethoxyphenol, methoxyvinylphenol, methoxypropenylphenol were detected with totalling concentrations ranging between 28 to 44.5 % of the identified compounds. The presence of the aforementioned phenol derivatives have resulted from the depolymerisation of lignin and its monomeric constituents, which according with the TGA analysis in Fig. 2, typically occur at temperatures between 400 and 600 °C (Mohan et al., 2006). Phenolic compounds can be used in the synthesis of bio-plastics, resins and epoxy polyurethane materials (Mamaeva et al., 2016).

Cellulose degradation is expected to occur at lower temperatures (usually between 240 - 350 °C) and results in the formation of anhydrocellulose and levoglucosan (Mohan et al., 2006)(Kostas et al., 2020)(Wu et al., 2009). Around 8.6 – 23.1 % of the total compounds identified in the generated bio-oils from this study was indeed levoglucosan, representing a valuable precursor fraction for conversion into plastics, surfactants, and bio-polymers (Rover et al., 2019). On the contrary, the main monomeric products from hemicellulose decomposition led to the formation of furfural and acetic acids, ranging between 13.2 to 25.2 %. Other compounds present in the bio-oils were aldehydes (6.5 – 12.4 %), methyl, vanillins and benzene and its derivatives (21.3 – 29.3 %).

Overall, the range of compounds identified in the bio-oil fractions generated in this study are comparable to bio-oils typically generated from lignocellulosic feedstock materials, offering wide opportunity for upgrading and incorporation bio-product manufacture (Pinheiro Pires et al., 2019).

Table 1. Semi-quantitative bio-oils composition of NS biomass.

Compound	Retention Time (min)	Percent of total identified (%)						
		I-N [300-3]	II-N [300-4]	III-N [300-5]	IV-N [300-6]	V-N [400-2]	VI-N [400-3]	VII-N [400-4]
Acetic acid	7.60	4.91	6.28	2.93	5.65	8.69	5.76	13.23
Furfural	12.64	8.28	6.99	4.47	8.18	13.47	11.48	11.95
Cyclopentanedione	15.99	1.30	1.32	1.36	1.27	1.27	1.23	1.49
Furanone	17.67	1.33	1.45	1.38	1.37	1.85	1.41	1.48
Oxazolidine, 2,2-diethyl-3-methyl-	18.34	5.04	4.58	5.50	4.69	5.88	5.35	7.98
Cyclopentanedione	18.97	3.46	2.98	2.95	2.99	3.68	3.10	3.44
Phenol	19.81	1.30	1.38	1.61	1.70	2.53	2.08	2.68
Methoxyphenol	20.40	7.87	5.23	5.42	4.64	5.68	4.94	6.66
Methylphenol	22.22	1.36	0.70	0.78	0.94	1.23	1.12	1.42
Methoxymethylphenol	23.33	9.85	6.39	7.66	6.14	6.81	6.57	8.09
Dimethylphenol	23.51	1.42	1.37	1.74	1.27	1.54	1.17	1.60
Ethylmethoxyphenol	25.62	2.75	1.45	1.76	0.32	0.40	1.57	1.77
Methoxyvinylphenol	27.10	2.86	2.19	3.16	3.04	2.81	3.20	3.42
Methoxypropenylphenol	27.77	2.09	1.26	1.46	1.28	1.40	1.42	1.70
Hydroxymethylfurancarboxaldehyde	28.11	3.13	1.88	2.41	2.04	2.59	2.01	2.48
Dimethoxyphenol	28.49	6.16	3.67	5.01	3.70	4.25	3.67	3.98
Methoxypropenylphenol	29.19	1.04	0.58	0.83	0.73	0.63	0.82	0.57
Methoxypropenylphenol	30.46	2.25	1.50	2.76	2.61	2.15	2.81	1.71
Trimethoxylbenzene	30.76	4.85	2.31	4.67	4.27	3.04	4.12	2.80
Vanillin	31.10	3.50	1.93	2.54	2.15	3.20	2.39	2.37
Methoxypropylphenol	32.47	1.93	1.01	1.42	1.05	0.64	0.11	0.74
Methyltrimethoxylbenzene	32.52	1.49	1.12	1.82	1.23	1.11	1.16	0.85
Hydroxymethyoxyphenyl	33.03	2.02	1.13	1.62	1.22	1.58	1.29	1.16
Hydroxymethoxyphenylpropanone	34.17	1.96	0.86	1.23	0.88	0.97	0.82	0.64
Dimethoxypropenylphenol	34.29	1.69	1.00	1.39	1.22	1.33	1.16	0.83
Hydroxymethoxyphenylpropanone	35.20	1.41	0.75	1.02	0.78	0.79	0.79	0.22
Levoglucosan	36.50	2.28	32.12	19.68	15.69	10.41	9.91	8.61
Dimethoxypropenylphenol	36.76	1.96	1.01	2.50	10.89	1.53	12.16	1.27
Hydroxydimethoxybenzealdehyde	37.49	2.10	1.32	1.91	1.57	1.80	1.46	1.19
Hydroxydimethoxyethanone	38.90	1.25	0.79	1.14	0.85	0.96	0.76	0.61
Hydroxymethoxycinnaanaldehyde	39.70	5.52	2.83	4.58	4.35	4.10	3.00	2.39
Dimethoxyhydroxycinnanaldehyde	44.66	1.64	0.62	1.30	1.29	1.68	1.16	0.68

*Preparation conditions [Power (W)-time (min)]

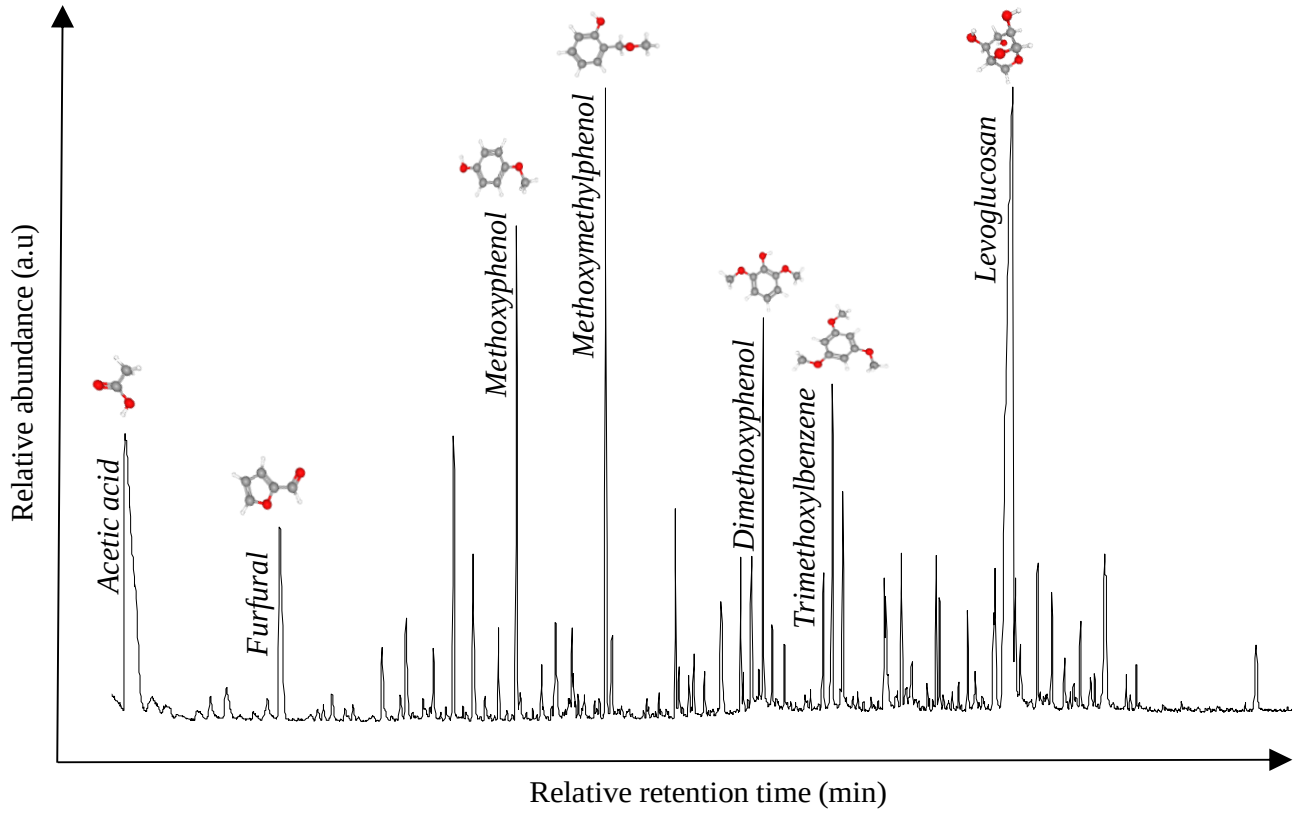

Fig. 3. GC-MS total ion chromatogram of a bio-oil sample (I-N) [300W-2min] generated from pecan NS microwave pyrolysis in this study.

Although the synthesis of bio-gas is beyond the scope of this work, attempts were made to analyse the non-condensable fraction obtained from the pyrolysis of biomass and it was found trace amounts of hydrogen (H_2) and methane (CH_4) (Fig. S3). Reasons for the trace levels could be due to the fact non catalyst were used in the process to maximize the bio-gas production (Weihong et al., 2019), but also due to that a relatively high nitrogen gas flow was applied in order to maintain an oxygen-free atmosphere and therefore aimed the dilution of gases produced. Despite the synthesis of bio-gas was not the main objective of this study, is important to highlight that studies have demonstrated the potential of NS for syngas production (Aldana et al., 2015), confirming the versatility and opportunities that this biomass offers for its valorisation.

3.3 Biochar characterisation

The elemental composition of the generated biochar samples is presented in Table 2, and show that regardless of the experimental conditions that were applied for the preparation of the biochars, biomass conversion into biochar was fully achieved as indicated by the carbon content ranging between 83.1 to 91.27 %. The hydrogen content (0.12 - 0.99 %), is associated with the small portion of compounds which remained in the solid carbon matrix. The biochars produced contained a high number of aromatic groups and relatively small aliphatic chains as indicated by a low H/C ratio, confirming that the aromaticity is due to dehydration, decarboxylation and cyclization reactions (Coromina et al., 2015). For all biochar samples, the carbon content increased for samples prepared at higher energies, for example VII-N has a specific energy of 8.4 kJ g^{-1} and a carbon content of 91.3 %, suggesting a higher level of graphitisation (See Tables 1 and 3).

The thermogravimetric profiles (TGA) of biochars are illustrated in Fig. S4. The weight losses observed from room temperature up to 110° C, are as result of the moisture removal. From 110 ° C all biochars showed a weight loss due to the volatile matter degradation. The proximate analysis is summarised in Table 2. The pecan NS has fixed carbon (10.8 %), volatile matter (84.4 %), moisture (3.6 %) and ash (1.3 %) (Durán-Jiménez et al., 2017). For the biochar, the data reveals a significant increase in fixed carbon whereas the volatile content shows a reversed trend. An increase in the microwave pyrolysis energy led to an increasing conversion to char, and reduction in the volatile matter. The increases observed in the fixed carbon and ash content as the pyrolysis energy increases could be due to the high temperature reached in the pyrolysis. The ash contents of the biochars were between 2.75 and 3.78 % and are a result of the transformation of the calcium oxalate in the precursor.

The elemental composition of biochar samples is consistent with the powder XRD patterns

shown in Fig. S5. An apparent increase in the intensity can be observed for the peaks at 2θ = 23 ° and 2θ = 43 °. Both peaks are ascribed to the diffraction of graphitic carbon domains (002) and (101) (Lahijani et al., 2018). The wide peak at 23 ° is associated with the highly disordered structure or amorphous carbon. The peak at 2θ = 43 ° correspond to the spacing between aromatic layers (Serafin et al., 2019). Additionally, the pecan NS biomass is rich in calcium in the form of oxalates ($CaC_2O_4 \cdot H_2O$), which progressively disappeared at higher microwave energy and at the time new peaks of $CaCO_3$ were formed in the biochar. This behaviour can be due to higher energies promote the decomposition of the oxalates, which is expected to occur at temperatures beyond 450 °C.

The morphology of the biochar prepared using a microwave power of 300 W for 6 min (IV-N) was analysed by SEM (Fig. S6 5 a-b) and EDX (Figs. S6 c-d). The morphology shows irregular cavities and pores (Fig. S6 a-b). The electron diffraction illustrates that the presence of superficial deposits composed of $CaCO_3$ (Fig. S6 c). The composition is validated by the XRD analysis (Fig. S5 b).

The textural parameters and the N_2 adsorption isotherms at -196 °C presented in Table 2 and Fig. S7. In general, the temperature required to devolatilise the biomass was successfully achieved after 3 min, thus enhancing the surface area and porosity of the biochar, whereas the largest specific surface area (187 m^2 g^{-1}) and the highest pore volume (0.075 cm^3 g^{-1}) were observed in the biochar prepared at 300 W for 6 min (300W -6 min). The results suggest that by increasing the microwave processing time to 6 min, the degree of micropore fraction also increases (85 %). The reduction in specific surface area and development of micropores along with the increase of specific energies (beyond 8 kJ g^{-1}), can be related to the disintegration of porous cavities as they are exposed to higher temperatures. Similar results have been previously reported for biochar prepared from similar biomass feedstocks such as walnut shells (Lahijani et al., 2018).

All biochars prepared exhibited a type I isotherm based on the IUPAC classification (Thommes, M., Kaneko, K., Neimark, A. V., 2015) (See Fig. S7) with high nitrogen uptake at low relative pressure (P/Po < 0.01); a feature that is characteristic of microporous materials (Choi et al., 2019). The widening of the knee of the isotherm in sample IV-N indicates a slight broadening of the micropore size range. The pore size distributions illustrate the higher micropore volume in the range of 0.33 to 0.44 nm and a small portion of 1.3 and 1.8 nm pores. The widening of the pore distribution in sample IV-N may be related to the controlled gasification of this particular biochar during pyrolysis at 6 min and 300 W. At powers of 400 W, a decrease in the textural properties was observed and may be related to the formation of hot spots which could lead to the detriment of pores by collapse of the pore walls (Huang et al., 2015).

3.4 Evaluation of biochar properties for CO_2 capture

The CO_2 uptake of the biochar produced was explored by volumetric analysis at 0 and 25 °C (Fig. 4). The simple-to-produce biochar in this study, present moderate CO_2 adsorption capacity at atmospheric pressure. The highest adsorption capacity of 2.5 and 2 mmol g^{-1} at 0 and 25 °C, respectively (Fig. 4) was obtained by the biochar (IV-N) produced at 300 W for 6 min of microwave heating making it superior to previously published biochars (Table S2, atmospheric pressure), such as rice straw (1.75 mmol g^{-1}) (Huang et al., 2015), sugar cane bagasse and hickory wood (1.67 & 1.32 mmol g^{-1}) (Creamer et al., 2014), walnut shell (1.65 mmol g^{-1}) (Lahijani et al., 2018), hickory chips (1.10 mmol g^{-1}) (Xu et al., 2019), pig manure and wheat straw (0.53 & 0.78 mmol g^{-1}) (Xu et al., 2016), mesquite wood and manure chicken (1.92 & 1.60 mmol g^{-1}) (Dissanayake et al., 2020).

The CO_2 adsorption results also indicate that biochars have higher CO_2 adsorption capacities than some activated carbons such as oil palm shell activated carbon (1.7 mmol g^{-1})

(Hoseinzadeh Hesas et al., 2015), pitch activated carbon (1.93 mmol g^{-1}) (Lee et al., 2014), olive stone activated carbon (1.40 – 1.98 mmol g^{-1}) (Plaza et al., 2014), soybean straw activated biochar with CO_2-NH_3 (1.86 mmol g^{-1}) (X. Zhang et al., 2016) and a number of metal organic frameworks materials, such as MIL-101(Cr) (1.98 mmol/g) (Lin et al., 2014). It is important to note the advanced materials such as activated carbons, have been reported to have higher CO_2 adsorption capacity, however biochars produced in this study were obtained without employing additional chemicals for doping or/and activation. This represents a potential alternative due to their effectiveness, eco-friendly nature, low cost and simple preparation.

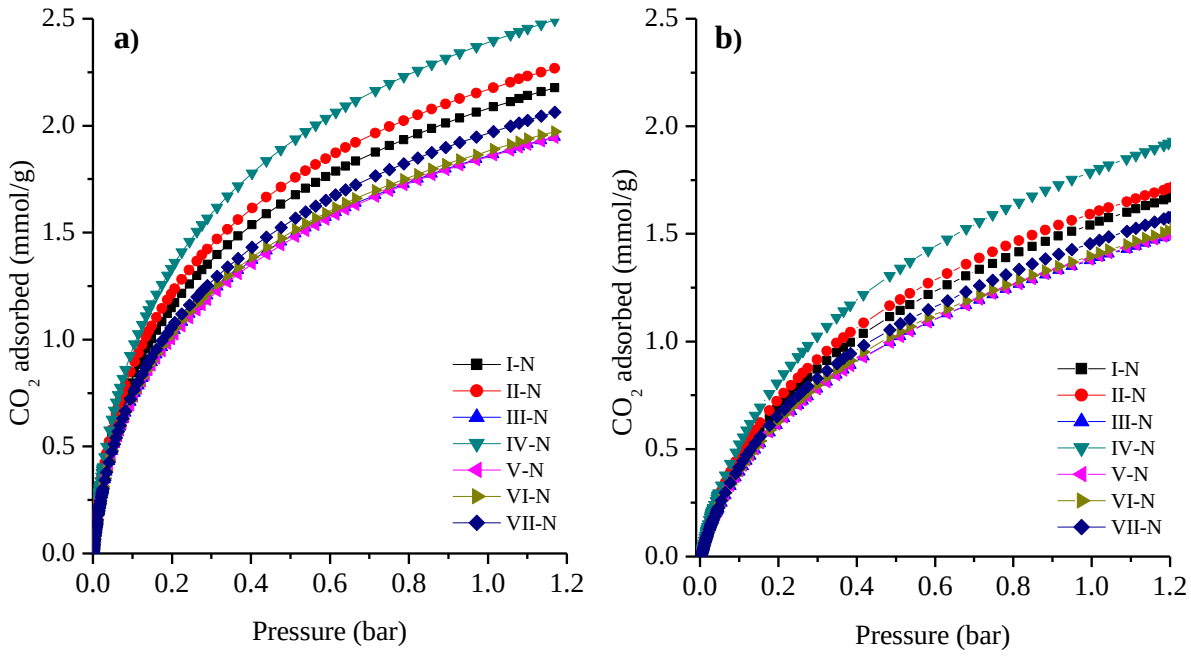

Fig. 4. CO_2 uptake at 0 (a) and 25 ° C (b) for biochars generated without activation from the microwave pyrolysis

Table 2. Elemental composition, proximate analysis and textural parameters of biochars obtained from microwave pyrolysis.

	Parameter (%)									Textural parameters			
Sample	**C**	**H**	**N**	**[a]O**	**H/C**	**Moisture**	**Volatile Matter**	**Fixed Carbon**	**Ash**	**[b]S_{BET} (m^2/g)**	**[c]V_p (cm^3/g)**	**[d]V_{mic} (cm^3/g)**	**V_{mes} (cm^3/g)**
I-N [300-3]	83.10	0.89	0.62	15.40	0.011	6.3	12.4	77.5	3.8	122	0.051	0.042	0.009
II-N [300-4]	86.58	0.83	0.80	11.79	0.010	5.2	8.6	82.4	3.7	151	0.062	0.05	0.012
III-N [300-5]	89.84	0.20	0.88	9.08	0.002	6.2	6.7	84.2	3.0	115	0.05	0.039	0.01
IV-N [300-6]	87.41	0.66	0.85	11.08	0.008	5.1	9.4	82.0	3.5	187	0.075	0.066	0.009
V-N [400-2]	83.56	0.99	0.51	14.94	0.012	6.0	7.1	84.2	2.8	42	0.02	0.017	0.003
VI-N [400-3]	87.1	0.37	0.82	11.71	0.004	4.7	9.0	82.5	3.7	134	0.057	0.047	0.01
VII-N [400-4]	91.27	0.12	0.97	7.64	0.001	4.1	6.1	86.6	3.3	112	0.048	0.038	0.01
NS	47.27	6.41	0.18	46.14	0.136	3.6	84.4	10.8	1.3	-	-	-	-

Preparation conditions [Power (W)-time (min)]

[a] Calculated by difference (%O=100-%C-%N-%H)

[b] BET surface area calculated by the BET method.

[c] Total pore volume recorded at 100 nm on cumulative pore volume by NLDFT carbon slit pore model.

[d] Micropore volume obtained at 2 nm on cumulative pore volume by NLDFT carbon slit pore model.

The CO_2 uptake capacity was correlated to the higher specific surface area and micropore volume. In our previous study, it was demonstrated that at pressures below to 1 bar, the CO_2 uptake is highly controlled by micropores with size below 0.7 nm (Durán-Jiménez et al., 2020). The results this work are also in agreement with the work published by Presser et al. (Presser et al., 2011) where was found that high surface area (> 2900 $m^2 g^{-1}$) with large total pore volume (> 1.5 $cm^3 g^{-1}$) is negligible for high CO_2 uptake and that high CO_2 adsorption will result in adsorbents with large narrow micropore volume. These findings are in correlation with the results shown in Fig. S8 that indicate the highest fraction of CO_2 filled pore occurs in pores of size of 0.7 nm, without further uptake increment for pores with size beyond 0.8 nm. This study confirms that pores larger than three times the molecular diameter of CO_2 (i.e. mesoporous materials) does not govern the CO_2 uptake at pre combustion conditions. The correlation of adsorbed amount with narrow micropores is fundamental in the design of effective and un-expensive adsorbents for industrial applications. Additionally, it is well-known the control of narrow micropores can be favourable to increase the CO_2 kinetics. This attribute in adsorbents is highly desirable for practical applications to reduce the required time of contact and energy for regeneration. Fig. 5 (a) presents the adsorption kinetics of biochar IV-N at 25 °C. It shows that levels of CO_2 adsorption up to 90 % can be achieved in less than 10 min, and fully equilibrate after 25 min.

To explore the potential of biochar for industrial applications, not only do the CO_2 uptake kinetics and mechanisms need to be considered, but also the CO_2 over N_2 selectivity, the isosteric heat of adsorption, adsorbent stability and recyclability ought to be investigated. The adsorbent's selectivity determines if the CO_2 can be removed from the flue gas mixture with minimal interference from other major gaseous species. In this study the selectivity of sample IV-N for CO_2 over N_2 was determined by thermogravimetric single component analysis at 25 °C at 1 bar (Durán-Jiménez et al., 2020). The CO_2 and N_2 uptake are compared in Fig. 5 (a).

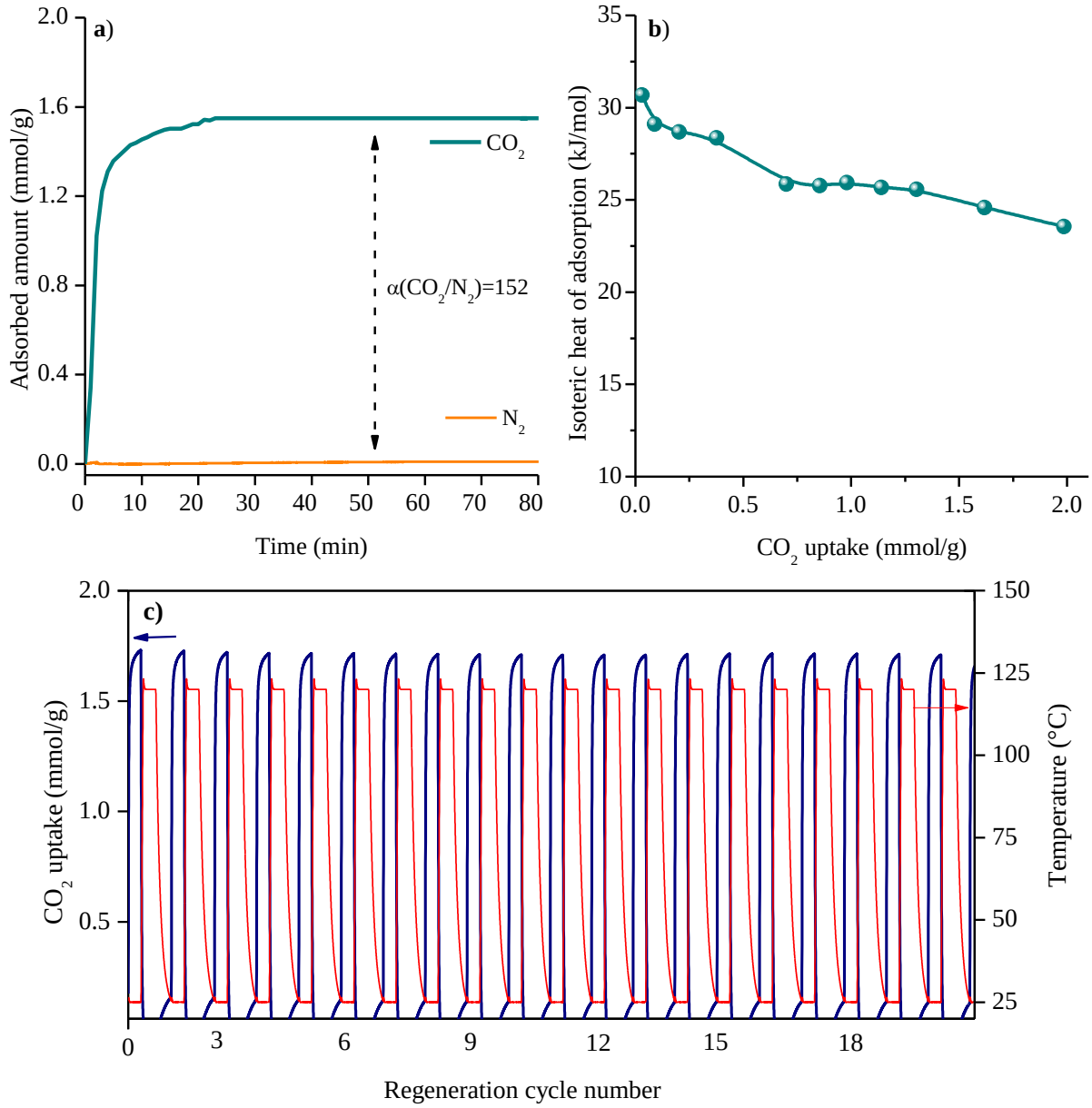

Fig. 5. CO_2 uptake kinetics & gas selectivity of biochar IV-N (a), Isoteric heat (Q_{st}) of CO_2 adsorption (b) and recyclability after 20 cycles of CO_2 IV-N at 25 °C (c)

The CO_2 uptake of IV-N (1.5 mmol g^{-1}) is distinctive higher than that of N_2 (0.001 mmol g^{-1}). The selectivity based on physisorption uptake, is dependent upon the different physical properties of gas molecules (Parshetti et al., 2015). Since the polarisability of CO_2 is higher than N_2, it is expected to have higher enthalpy of adsorption which leads to a higher affinity of the pore surface, and therefore a higher selectivity. It should also be noted that the selectivity

reported in this study is higher than recently reported porous carbon materials (Li and Xiao, 2019)(Lahijani et al., 2018)(Chen et al., 2018), indicating that the biochar produced in this study could be implemented for gas separation in practical applications.

The high CO_2/N_2 selectivity of IV-N is also supported by the high isosteric heats of adsorption shown in Fig. 5 (b) calculated applying the Clausius-Clapeyron equation (Durán-Jiménez et al., 2020). The relatively high initial Q_{st} values in the low-pressure region, suggest the CO_2 molecules are being adsorbed on sites with the highest energy and narrowest micropores. At higher CO_2 uptake, the Q_{st} values decay below 30 kJ mol^{-1} indicating the CO_2 adsorption is governed by the physisorption mechanism. The values reported for sample IV-N are similar to values reported for porous carbon materials (Chen et al., 2018) (Hong et al., 2016).

It is essential to evaluate the regeneration and reusability of the adsorbents to assess its further industrial implementation. Fig. 5c) shows the CO_2 adsorption - desorption cycles of the IV-N biochar at 100 % CO_2. It can be seen that after twenty consecutive cycles the CO_2 adsorption kinetics and equilibrium uptake remained unaffected, confirming the stability and easy regeneration. This result demonstrates the high chemical and physical stability of biochar and confirms the adsorption is reversible governed by mechanisms of the physi-sorption.

4 Conclusions

This work has demonstrated that a range of desireable bio-products with further applications can be effectively synthesised from pecan NS waste biomass employing only 6 min of microwave heating. The yields of the pyrolysis products were found to be greatly influenced by microwave energy and processing parameters, and 8 kJ g^{-1} of energy was required to obtain 39 % of bio-oil that contains upgradeable chemical compounds such as levoglucosan, phenols, and furfural. The results also revealed unique characteristics of the generated biochars, such as pore size distribution and ultra-micropores being the main responsible parameter for the post-

combustion CO_2 uptake. The values reported herein (2.5 mmol CO_2 g^{-1}) are competitive or higher than other values reported for other biochars, which include: significantly greater CO_2 uptake over N_2 and easy regeneration. These findings are of significant importance, not only due to the competitive properties of biochar and due to its application in the CO_2 capture, but also because it offers a greener and simple approach using microwave heating. Furthermore, no doping agents were used in the synthesis methodology that was employed, making it a great sustainable alternative for waste disposal.

Acknowledgements

This research was supported by the Council of Science and Technology (CONACyT), Mexico under the grant 389535.

5 References

Acevedo-García, V., Rosales, E., Puga, A., Pazos, M., Sanromán, M.A., 2020. Synthesis and use of efficient adsorbents under the principles of circular economy: Waste valorisation and electroadvanced oxidation process regeneration. Sep. Purif. Technol. 242, 116796. https://doi.org/10.1016/j.seppur.2020.116796

Adeniran, B., Masika, E., Mokaya, R., 2014. A family of microporous carbons prepared via a simple metal salt carbonization route with high selectivity for exceptional gravimetric and volumetric post-combustion CO2 capture. J. Mater. Chem. A 2, 14696–14710. https://doi.org/10.1039/c4ta03565h

Agustin-Salazar, S., Cerruti, P., Medina-Juárez, L.Á., Scarinzi, G., Malinconico, M., Soto-Valdez, H., Gamez-Meza, N., 2018. Lignin and holocellulose from pecan nutshell as reinforcing fillers in poly (lactic acid) biocomposites. Int. J. Biol. Macromol. 115, 727–736. https://doi.org/10.1016/j.ijbiomac.2018.04.120

Aldana, H., Lozano, F.J., Acevedo, J., Mendoza, A., 2015. Thermogravimetric characterization and gasification of pecan nut shells. Bioresour. Technol. 198, 634–641. https://doi.org/10.1016/j.biortech.2015.09.069

Almustapha, M.N., Farooq, M., Andresen, J.M., 2017. Sulphated zirconia catalysed conversion of high density polyethylene to value-added products using a fixed-bed reactor. J. Anal. Appl. Pyrolysis 125, 296–303. https://doi.org/10.1016/j.jaap.2017.03.013

Beneroso, D., Monti, T., Kostas, E.T., Robinson, J., 2017. Microwave pyrolysis of biomass for bio-oil production: Scalable processing concepts. Chem. Eng. J. 316, 481–498. https://doi.org/10.1016/j.cej.2017.01.130

Bui Viet, D., Chan, W.P., Phua, Z.H., Ebrahimi, A., Abbas, A., Lisak, G., 2020. The use of fly ashes from waste-to-energy processes as mineral CO2 sequesters and supplementary cementitious materials. J. Hazard. Mater. 398, 122906. https://doi.org/10.1016/j.jhazmat.2020.122906

Chen, C., Huang, H., Yu, Y., Shi, J., He, C., Albilali, R., Pan, H., 2018. Template-free synthesis of hierarchical porous carbon with controlled morphology for CO2 efficient capture. Chem. Eng. J. 353, 584–594. https://doi.org/10.1016/j.cej.2018.07.161

Choi, S.W., Tang, J., Pol, V.G., Lee, K.B., 2019. Pollen-derived porous carbon by KOH activation: Effect of physicochemical structure on CO 2 adsorption. J. CO2 Util. 29, 146–155. https://doi.org/10.1016/j.jcou.2018.12.005

Coromina, H.M., Walsh, D.A., Mokaya, R., 2015. Biomass-derived activated carbon with simultaneously enhanced CO2 uptake for both pre and post combustion capture applications. J. Mater. Chem. A 4, 280–289. https://doi.org/10.1039/c5ta09202g

Creamer, A.E., Gao, B., Zhang, M., 2014. Carbon dioxide capture using biochar produced from sugarcane bagasse and hickory wood. Chem. Eng. J. 249, 174–179. https://doi.org/10.1016/j.cej.2014.03.105

Dissanayake, P.D., Choi, S.W., Igalavithana, A.D., Yang, X., Tsang, D.C.W., Wang, C.H., Kua, H.W., Lee, K.B., Ok, Y.S., 2020. Sustainable gasification biochar as a high efficiency adsorbent for CO2 capture: A facile method to designer biochar fabrication. Renew. Sustain. Energy Rev. 124, 109785. https://doi.org/10.1016/j.rser.2020.109785

Donahue, C.J., Rais, E.A., 2009. Proximate Analysis of Leucaena Leucocephala (Lam.) De Wit, Parkia Biglobosa (Jacq.) Benth and Prosopis Africana (Guill & Perr.) Taub. J. Chem. Educ. 86, 222. https://doi.org/10.1021/ed086p222

Durán-Jiménez, G., Hernández-Montoya, V., Montes-Morán, M.A., Rangel-Méndez, J.R., Tovar-Gómez, R., 2016. Study of the adsorption-desorption of Cu2 +, Cd2 + and Zn2 + in single and binary aqueous solutions using oxygenated carbons prepared by Microwave Technology. J. Mol. Liq. 220, 855–864. https://doi.org/10.1016/j.molliq.2016.05.027

Durán-Jiménez, G., Hernández-Montoya, V., Montes-Morán, M.A., Teutli-León, M., 2015. New oxygenated carbonaceous adsorbents prepared by combined radiant/microwave heating for the removal of Pb2+ in aqueous solution. J. Anal. Appl. Pyrolysis 113, 599–605. https://doi.org/10.1016/j.jaap.2015.04.001

Durán-Jiménez, G., Monti, T., Titman, J.J., Hernandez-Montoya, V., Kingman, S.W., Binner, E.R., 2017. New insights into microwave pyrolysis of biomass: Preparation of carbon-

based products from pecan nutshells and their application in wastewater treatment. J. Anal. Appl. Pyrolysis 124, 113–121. https://doi.org/10.1016/j.jaap.2017.02.013

Durán-Jiménez, G., Stevens, L.A., Kostas, E.T., Hernández-Montoya, V., Robinson, J.P., Binner, E.R., 2020. Rapid, simple and sustainable synthesis of ultra-microporous carbons with high performance for CO2 uptake, via microwave heating. Chem. Eng. J. 388, 124309. https://doi.org/10.1016/j.cej.2020.124309

Ferrera-Lorenzo, N., Fuente, E., Suárez-Ruiz, I., Gil, R.R., Ruiz, B., 2014. Pyrolysis characteristics of a macroalgae solid waste generated by the industrial production of Agar–Agar. J. Anal. Appl. Pyrolysis 105, 209–216.

Haeldermans, T., Claesen, J., Maggen, J., Carleer, R., Yperman, J., Adriaensens, P., Samyn, P., Vandamme, D., Cuypers, A., Vanreppelen, K., Schreurs, S., 2019. Microwave assisted and conventional pyrolysis of MDF – Characterization of the produced biochars. J. Anal. Appl. Pyrolysis 138, 218–230. https://doi.org/10.1016/j.jaap.2018.12.027

Hong, S.M., Choi, S.W., Kim, S.H., Lee, K.B., 2016. Porous carbon based on polyvinylidene fluoride: Enhancement of CO2 adsorption by physical activation. Carbon N. Y. 99, 354–360. https://doi.org/10.1016/j.carbon.2015.12.012

Hoseinzadeh Hesas, R., Arami-Niya, A., Wan Daud, W.M.A., Sahu, J.N., 2015. Microwave-assisted production of activated carbons from oil palm shell in the presence of CO2 or N2 for CO2 adsorption. J. Ind. Eng. Chem. 24, 196–205. https://doi.org/10.1016/j.jiec.2014.09.029

Huang, Y.F., Chiueh, P. Te, Shih, C.H., Lo, S.L., Sun, L., Zhong, Y., Qiu, C., 2015. Microwave pyrolysis of rice straw to produce biochar as an adsorbent for CO2 capture. Energy 84, 75–82. https://doi.org/10.1016/j.energy.2015.02.026

Jung, S., Park, Y.K., Kwon, E.E., 2019. Strategic use of biochar for CO2 capture and sequestration. J. CO2 Util. 32, 128–139. https://doi.org/10.1016/j.jcou.2019.04.012

Kan, T., Strezov, V., Evans, T.J., 2016. Lignocellulosic biomass pyrolysis: A review of product properties and effects of pyrolysis parameters. Renew. Sustain. Energy Rev. 57, 1126–1140. https://doi.org/10.1016/j.rser.2015.12.185

Kostas, E.T., Beneroso, D., Robinson, J.P., 2017. The application of microwave heating in bioenergy: A review on the microwave pre-treatment and upgrading technologies for biomass. Renew. Sustain. Energy Rev. 77, 12–27. https://doi.org/10.1016/j.rser.2017.03.135

Kostas, E.T., Durán-Jiménez, G., Shepherd, B.J., Meredith, W., Stevens, L.A., Williams, O.S.A., Lye, G.J., Robinson, J.P., 2020. Microwave pyrolysis of olive pomace for bio-oil and bio-char production. Chem. Eng. J. 387, 123404. https://doi.org/10.1016/j.cej.2019.123404

Kostas, E.T., Williams, O.S.A., Duran-Jimenez, G., Tapper, A.J., Cooper, M., Meehan, R., Robinson, J.P., 2019. Microwave pyrolysis of Laminaria digitata to produce unique seaweed-derived bio-oils. Biomass and Bioenergy 125, 41–49. https://doi.org/10.1016/j.biombioe.2019.04.006

Lahijani, P., Mohammadi, M., Mohamed, A.R., 2018. Metal incorporated biochar as a potential adsorbent for high capacity CO2 capture at ambient condition. J. CO2 Util. 26, 281–293. https://doi.org/10.1016/j.jcou.2018.05.018

Lee, S.Y., Yoo, H.M., Park, S.W., Hee Park, S., Oh, Y.S., Rhee, K.Y., Park, S.J., 2014. Preparation and characterization of pitch-based nanoporous carbons for improving CO2 capture. J. Solid State Chem. 215, 201–205. https://doi.org/10.1016/j.jssc.2014.03.038

Li, J., Dai, J., Liu, G., Zhang, H., Gao, Z., Fu, J., He, Y., Huang, Y., 2016. Biochar from microwave pyrolysis of biomass: A review. Biomass and Bioenergy 94, 228–244. https://doi.org/10.1016/j.biombioe.2016.09.010

Li, M., Xiao, R., 2019. Preparation of a dual Pore Structure Activated Carbon from Rice Husk Char as an Adsorbent for CO2 Capture. Fuel Process. Technol. 186, 35–39. https://doi.org/10.1016/j.fuproc.2018.12.015

Li, W., Dang, Q., Brown, R.C., Laird, D., Wright, M.M., 2017. The impacts of biomass properties on pyrolysis yields, economic and environmental performance of the pyrolysis-bioenergy-biochar platform to carbon negative energy. Bioresour. Technol. 241, 959–968. https://doi.org/10.1016/j.biortech.2017.06.049

Li, Y., Ruan, G., Jalilov, A.S., Tarkunde, Y.R., Fei, H., Tour, J.M., 2016. Biochar as a renewable source for high-performance CO2 sorbent. Carbon N. Y. 107, 344–351. https://doi.org/10.1016/j.carbon.2016.06.010

Liang, Z., Marshall, M., Chaffee, A.L., 2009. CO2 adsorption-based separation by metal organic framework (Cu-BTC) versus zeolite (13X). Energy and Fuels 23, 2785–2789. https://doi.org/10.1021/ef800938e

Lin, Y., Lin, H., Wang, H., Suo, Y., Li, B., Kong, C., Chen, L., 2014. Enhanced selective CO2 adsorption on polyamine/MIL-101(Cr) composites. J. Mater. Chem. A 2, 14658–14665. https://doi.org/10.1039/c4ta01174k

Lozano, F.J., Lozano, R., 2018. Assessing the potential sustainability benefits of agricultural residues: Biomass conversion to syngas for energy generation or to chemicals production. J. Clean. Prod. 172, 4162–4169. https://doi.org/10.1016/j.jclepro.2017.01.037

Mamaeva, A., Tahmasebi, A., Tian, L., Yu, J., 2016. Microwave-assisted catalytic pyrolysis of lignocellulosic biomass for production of phenolic-rich bio-oil. Bioresour. Technol. 211, 382–389. https://doi.org/10.1016/j.biortech.2016.03.120

Martínez-Casillas, D.C., Mascorro-Gutiérrez, I., Arreola-Ramos, C.E., Villafán-Vidales, H.I., Arancibia-Bulnes, C.A., Ramos-Sánchez, V.H., Cuentas-Gallegos, A.K., 2019. A sustainable approach to produce activated carbons from pecan nutshell waste for environmentally friendly supercapacitors. Carbon N. Y. 148, 403–412. https://doi.org/10.1016/j.carbon.2019.04.017

Miura, M., Kaga, H., Sakurai, A., Kakuchi, T., Takahashi, K., 2004. Rapid pyrolysis of wood block by microwave heating. J. Anal. Appl. Pyrolysis 71, 187–199. https://doi.org/10.1016/S0165-2370(03)00087-1

Mohan, D., Pittman, C.U., Steele, P.H., 2006. Pyrolysis of wood/biomass for bio-oil: A critical review. Energy and Fuels 20, 848–889. https://doi.org/10.1021/ef0502397

Nagahata, R., Takeuchi, K., 2019. Encouragements for the Use of Microwaves in Industrial Chemistry. Chem. Rec. 19, 51–64. https://doi.org/10.1002/tcr.201800064

Namazi, A.B., Allen, D.G., Jia, C.Q., 2015. Probing microwave heating of lignocellulosic biomasses. J. Anal. Appl. Pyrolysis 112, 121–128. https://doi.org/10.1016/j.jaap.2015.02.009

Nations, U. Paris Agreement to the United Nations Framework Convention on Climate Change, 2015.

Olabi, A.G., 2019. Circular economy and renewable energy. Energy 181, 450–454. https://doi.org/10.1016/j.energy.2019.05.196

Parshetti, G.K., Chowdhury, S., Balasubramanian, R., 2015. Biomass derived low-cost microporous adsorbents for efficient CO2 capture. Fuel 148, 246–254. https://doi.org/10.1016/j.fuel.2015.01.032

Pinheiro Pires, A.P., Arauzo, J., Fonts, I., Domine, M.E., Fernández Arroyo, A., Garcia-Perez, M.E., Montoya, J., Chejne, F., Pfromm, P., Garcia-Perez, M., 2019. Challenges and opportunities for bio-oil refining: A review. Energy and Fuels 33, 4683–4720. https://doi.org/10.1021/acs.energyfuels.9b00039

Plaza, M.G., González, A.S., Pis, J.J., Rubiera, F., Pevida, C., 2014. Production of microporous biochars by single-step oxidation: Effect of activation conditions on CO2 capture. Appl. Energy 114, 551–562. https://doi.org/10.1016/j.apenergy.2013.09.058

Presser, V., Mcdonough, J., Yeon, S., Gogotsi, Y., 2011. Effect of pore size on carbon dioxide sorption by carbide derived carbon. Energy Environ. Sci. 3059–3066. https://doi.org/10.1039/c1ee01176f

Rover, M.R., Aui, A., Wright, M.M., Smith, R.G., Brown, R.C., 2019. Production and purification of crystallized levoglucosan from pyrolysis of lignocellulosic biomass. Green Chem. 21, 5980–5989. https://doi.org/10.1039/c9gc02461a

Saha, D., Bao, Z., Jia, F., Deng, S., 2010. Adsorption of CO2, CH4, N2O, and N 2 on MOF-5, MOF-177, and zeolite 5A. Environ. Sci. Technol. 44, 1820–1826. https://doi.org/10.1021/es9032309

Sanna, A., Dri, M., Hall, M.R., Maroto-Valer, M., 2012. Waste materials for carbon capture and storage by mineralisation (CCSM) - A UK perspective. Appl. Energy 99, 545–554. https://doi.org/10.1016/j.apenergy.2012.06.049

Santos, M.S.N. do., Zabot, G.L., Mazutti, M.A., Ugalde, G.A., Rezzadori, K., Tres, M. V., 2020. Optimization of subcritical water hydrolysis of pecan wastes biomasses in a semi-continuous mode. Bioresour. Technol. 306, 123129. https://doi.org/10.1016/j.biortech.2020.123129

Sears, K.E., Behringer, R.R., Rasweiler, J.J. 4th, Niswander, L.A., 2006. Development of bat flight: morphologic and molecular evolution of bat wing digits. Proc. Natl. Acad. Sci. U. S. A. 103, 6581–6586. https://doi.org/10.1073/pnas.0509716103

Serafin, J., Baca, M., Biegun, M., Mijowska, E., Kaleńczuk, R.J., Sreńscek-Nazzal, J., Michalkiewicz, B., 2019. Direct conversion of biomass to nanoporous activated biocarbons for high CO2 adsorption and supercapacitor applications. Appl. Surf. Sci. 497. https://doi.org/10.1016/j.apsusc.2019.143722

Singh, G., Lakhi, K.S., Sil, S., Bhosale, S. V., Kim, I.Y., Albahily, K., Vinu, A., 2019. Biomass derived porous carbon for CO 2 capture. Carbon N. Y. 148, 164–186. https://doi.org/10.1016/j.carbon.2019.03.050

Srinivas, G., Krungleviciute, V., Guo, Z.X., Yildirim, T., 2014. Exceptional CO2 capture in a hierarchically porous carbon with simultaneous high surface area and pore volume. Energy Environ. Sci. 7, 335–342. https://doi.org/10.1039/c3ee42918k

Thommes, M., Kaneko, K., Neimark, A. V., et al., 2015. Physisorption of gases, with special reference to the evaluation of surface area and pore size distribution (IUPAC Technical Report).

Thommes, M., Kaneko, K., Neimark, A. V., Olivier, J.P., Rodriguez-Reinoso, F., Rouquerol, J., Sing, K.S.W., 2015. Physisorption of gases, with special reference to the evaluation of surface area and pore size distribution (IUPAC Technical Report). Pure Appl. Chem. 87, 1051–1069. https://doi.org/10.1515/pac-2014-1117

Weihong, Z., Bin, B., Guanyi, C., Longlong, M., Beibei, Y., 2019. Thermogravimetric characteristics and kinetics of sawdust pyrolysis catalyzed by potassium salt during the process of hydrogen preparation. Int. J. Hydrogen Energy 44, 15863–15870. https://doi.org/10.1016/j.ijhydene.2019.01.060

Wu, Y.M., Zhao, Z.L., Li, H. Bin, He, F., 2009. Low temperature pyrolysis characteristics of major components of biomass. Ranliao Huaxue Xuebao/Journal Fuel Chem. Technol. 37, 427–432. https://doi.org/10.1016/s1872-5813(10)60002-3

Xu, X., Kan, Y., Zhao, L., Cao, X., 2016. Chemical transformation of CO2 during its capture by waste biomass derived biochars. Environ. Pollut. 213, 533–540. https://doi.org/10.1016/j.envpol.2016.03.013

Xu, X., Zheng, Y., Gao, B., Cao, X., 2019. N-doped biochar synthesized by a facile ball-milling method for enhanced sorption of CO2 and reactive red. Chem. Eng. J. 368, 564–572. https://doi.org/10.1016/j.cej.2019.02.165

Yang, J., Yue, L., Hu, X., Wang, L., Zhao, Y., Lin, Y., Sun, Y., DaCosta, H., Guo, L., 2017. Efficient CO2 Capture by Porous Carbons Derived from Coconut Shell. Energy and Fuels 31, 4287–4293. https://doi.org/10.1021/acs.energyfuels.7b00633

Yin, C., 2012. Microwave-assisted pyrolysis of biomass for liquid biofuels production. Bioresour. Technol. 120, 273–284. https://doi.org/10.1016/j.biortech.2012.06.016

Zappa, W., Junginger, M., van den Broek, M., 2019. Is a 100% renewable European power system feasible by 2050? Appl. Energy 233–234, 1027–1050. https://doi.org/10.1016/j.apenergy.2018.08.109

Zhang, C., Song, W., Ma, Q., Xie, L., Zhang, X., Guo, H., 2016. Enhancement of CO2 Capture on Biomass-Based Carbon from Black Locust by KOH Activation and Ammonia Modification. Energy and Fuels 30, 4181–4190. https://doi.org/10.1021/acs.energyfuels.5b02764

Zhang, X., Wu, J., Yang, H., Shao, J., Wang, X., Chen, Y., Zhang, S., Chen, H., 2016. Preparation of nitrogen-doped microporous modified biochar by high temperature CO2-NH3 treatment for CO2 adsorption: Effects of temperature. RSC Adv. 6, 98157–98166. https://doi.org/10.1039/c6ra23748g

GRAPHICAL ABSTRACT

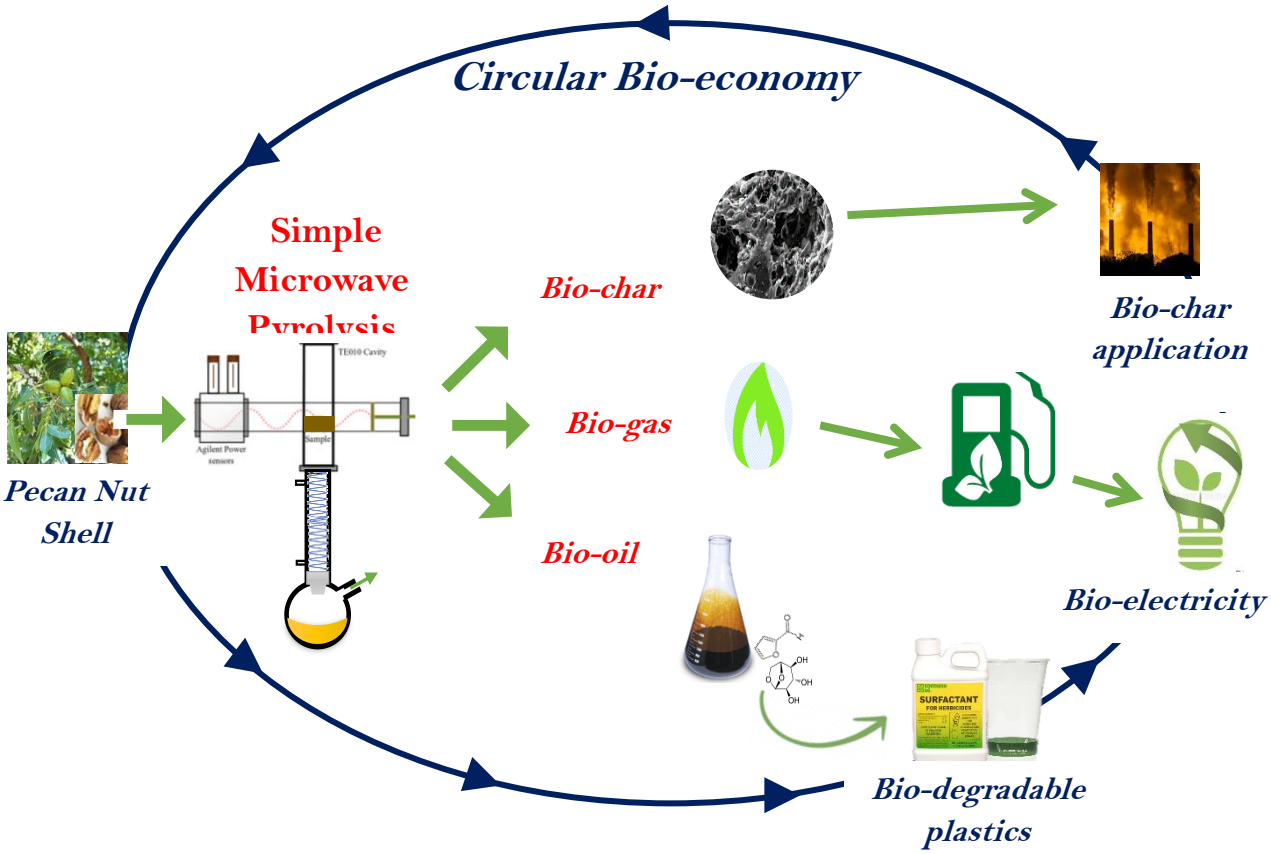

SUPPLEMENTARY INFORMATION

Figures

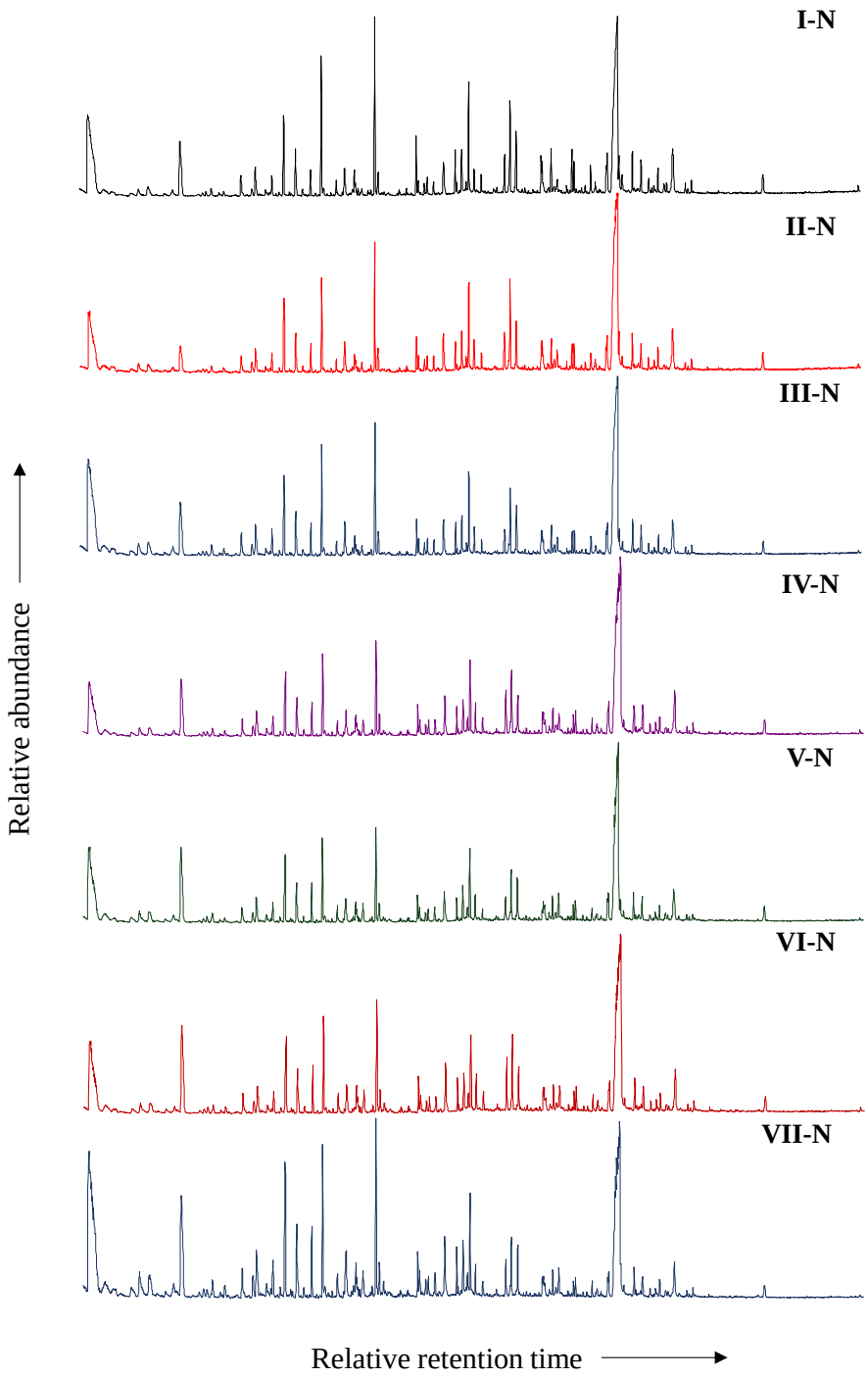

Fig. S1. GC-MS Chromatograms of bio-oil produced from microwave biomass pyrolysis.

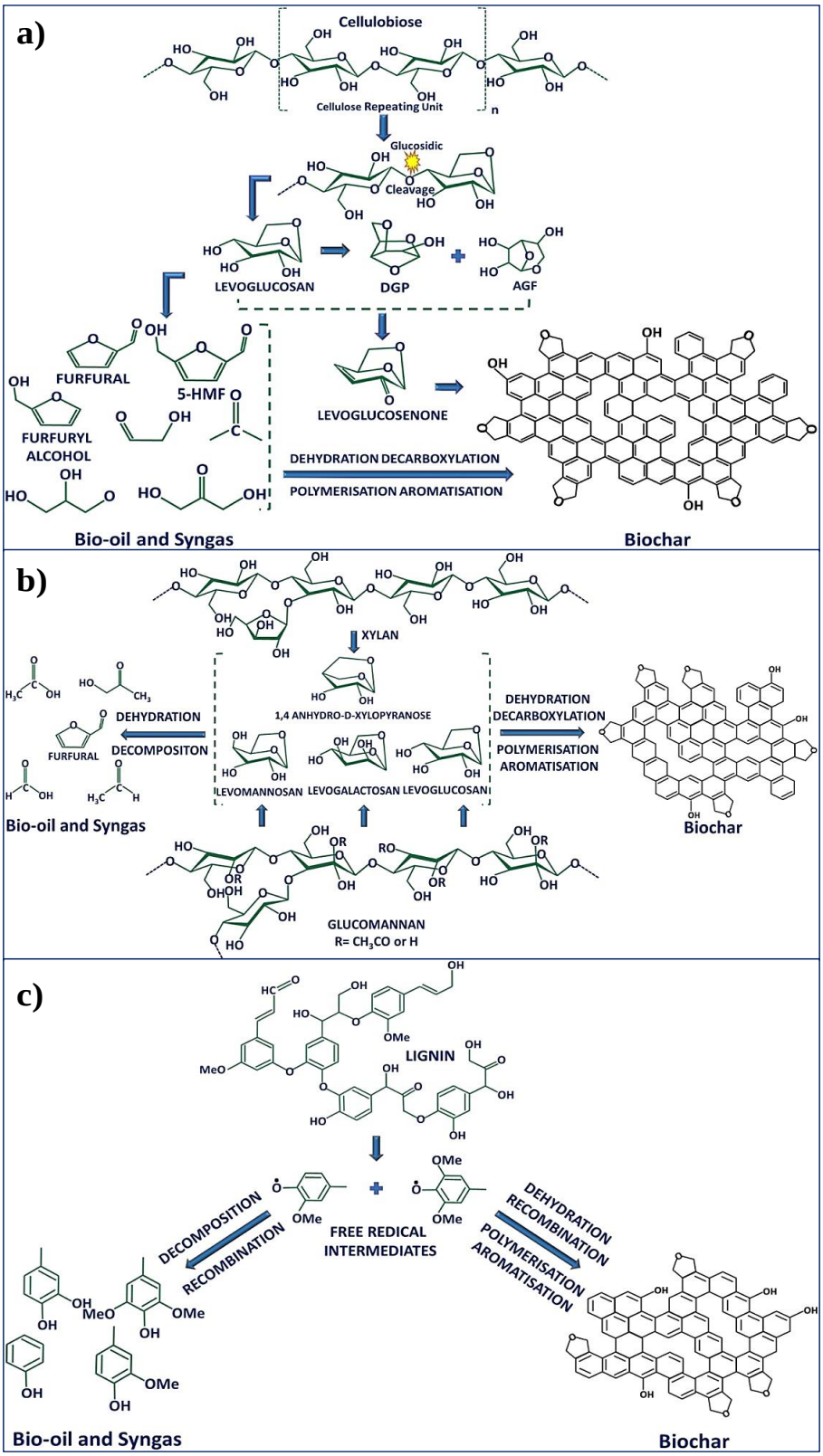

Fig. S2. Pyrolysis mechanism of cellulose (a), hemicellulose (b) and lignin (c) in the formation of bio-oil and bio-char. With permission from (Singh et al., 2019) License Number (4934750662635).

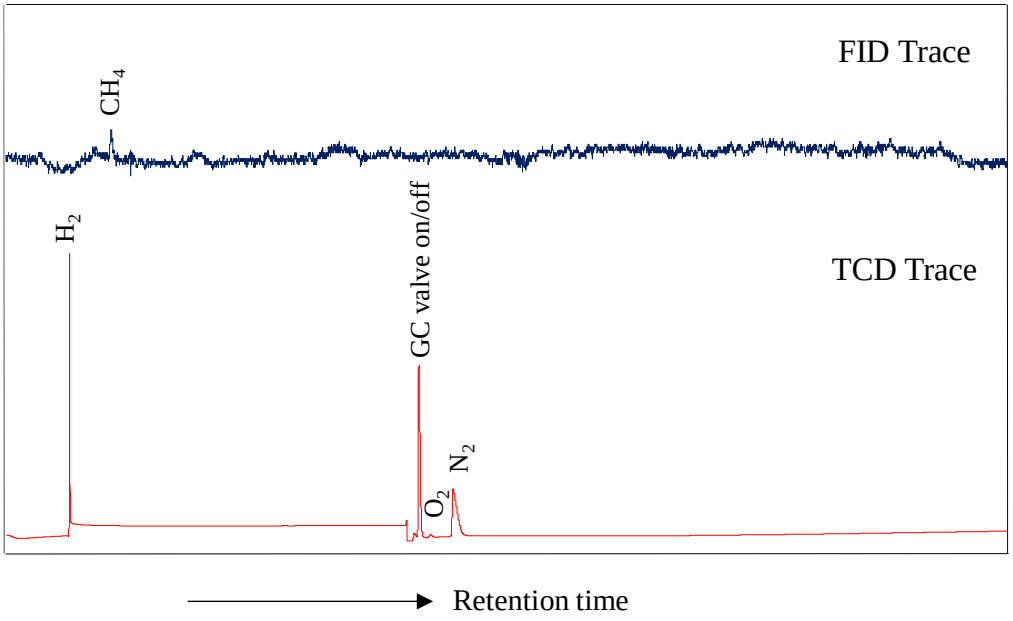

Fig. S3. Gas chromatogram of I-NS bio-gas sample

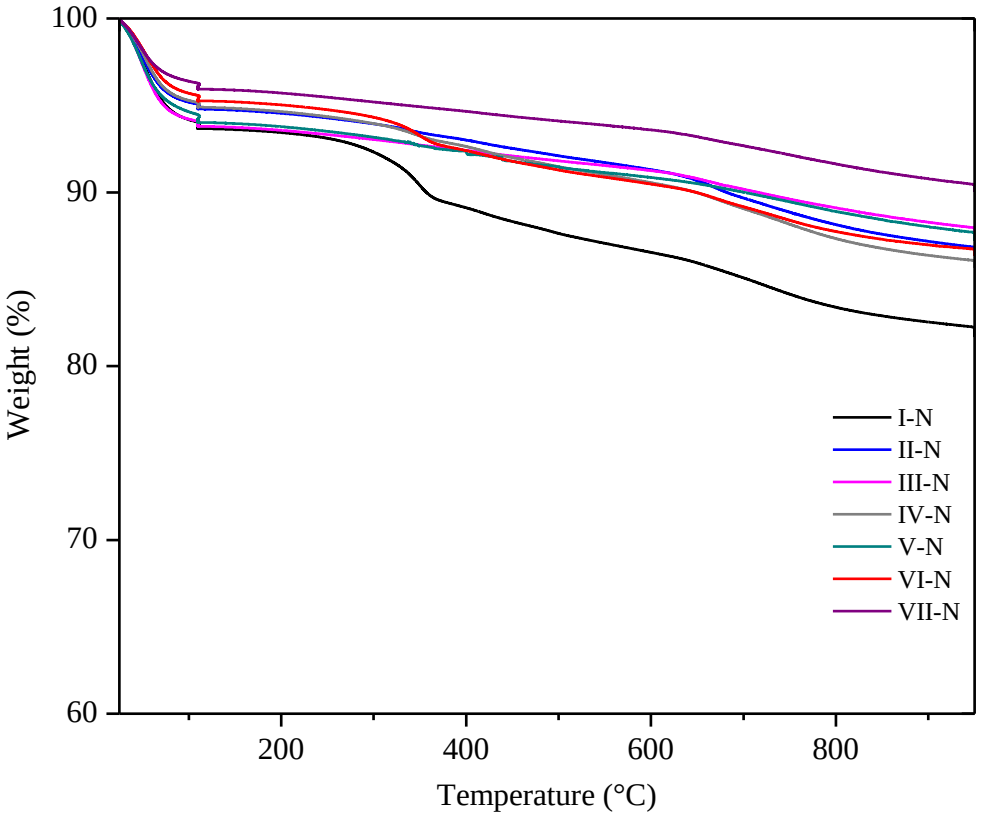

Fig. S4. TGA curves of bio-chars

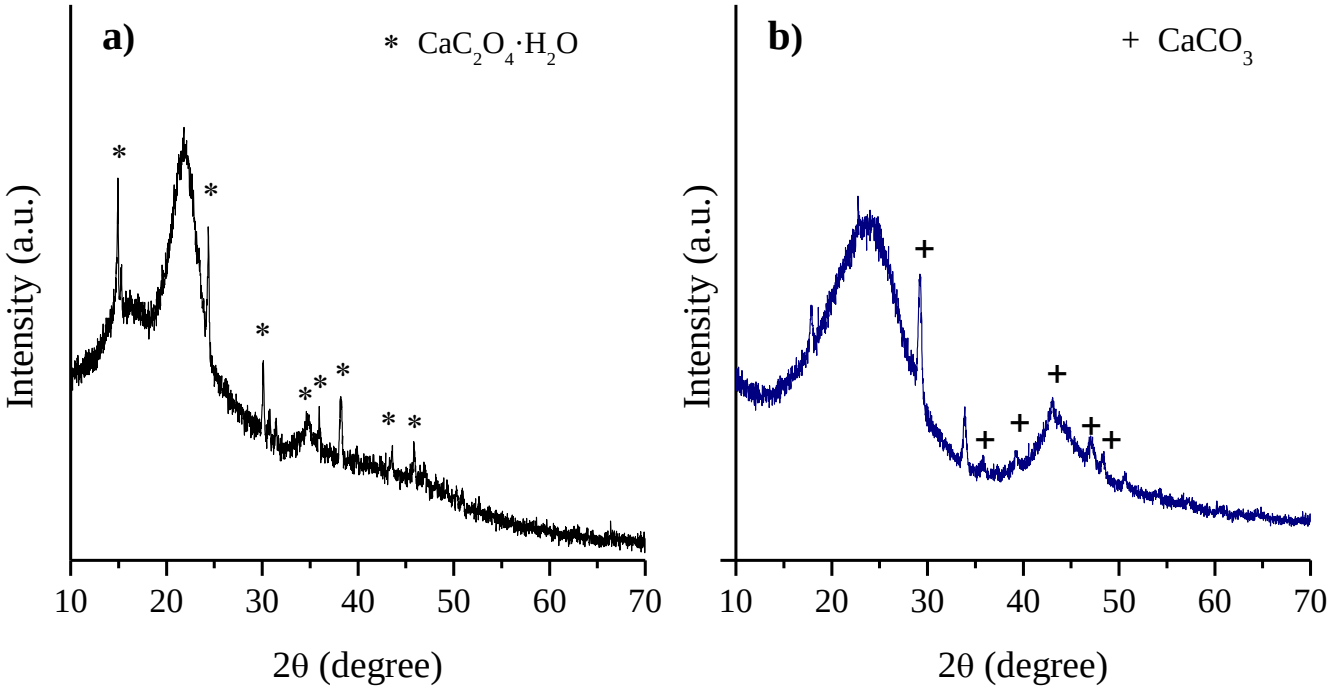

Fig. S5. XRD patterns of pecan NS biomass (a) and bio-char IV-N prepared by the microwave pyrolysis.

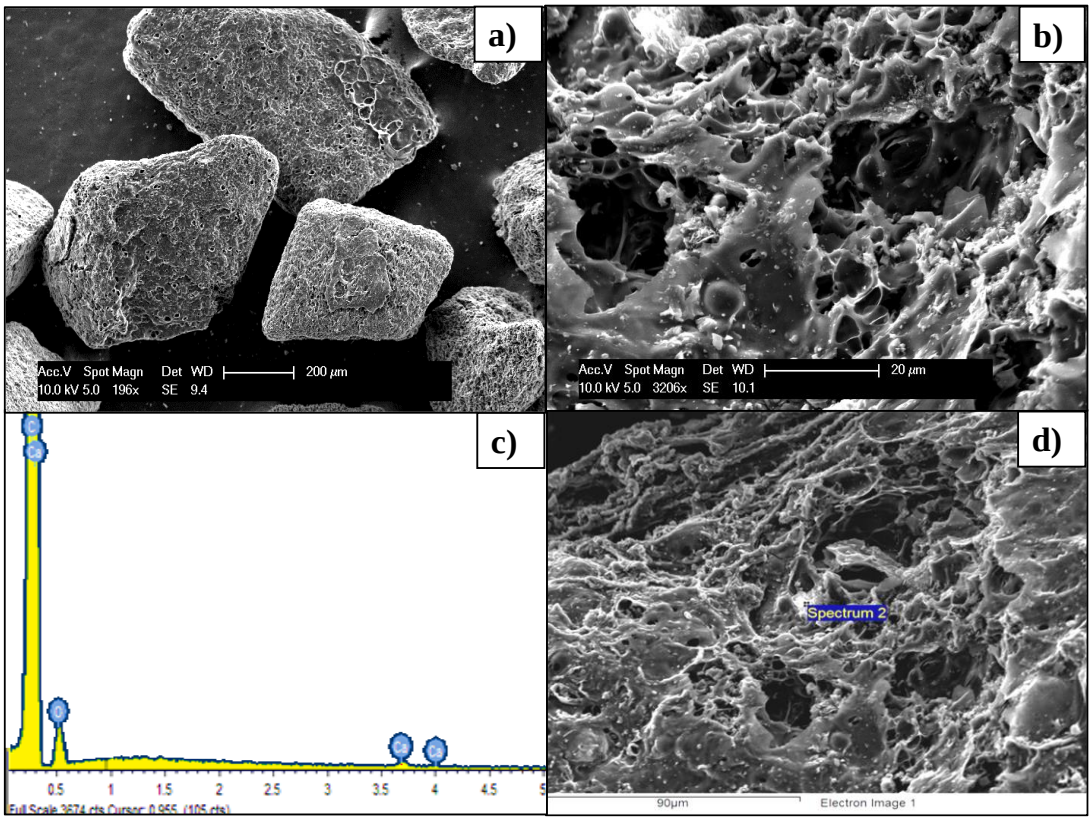

Fig. S6. SEM images (a-b) at different scales and EDX (c-d) of IV-N bio-char, which was

prepared using microwave pyrolysis conditions of 300 W for 6 min.

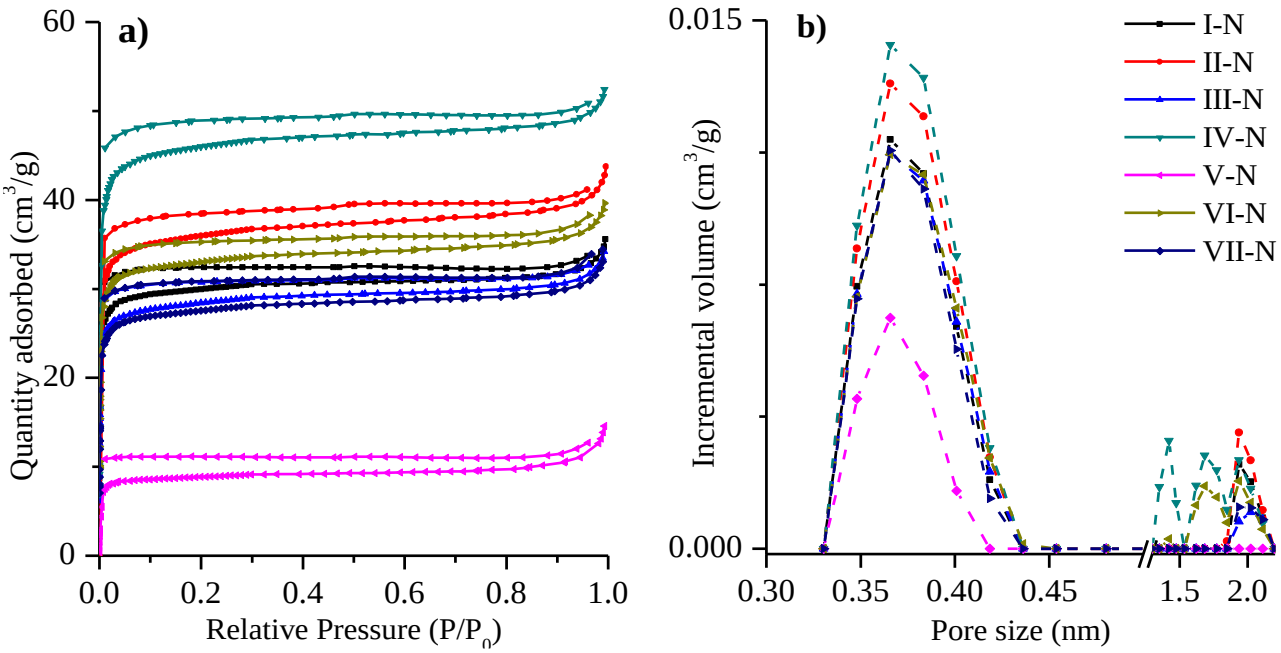

Fig. S7. Nitrogen adsorption-desorption isotherms (a) and pore size distribution (b) of bio-chars prepared by microwave pyrolysis.

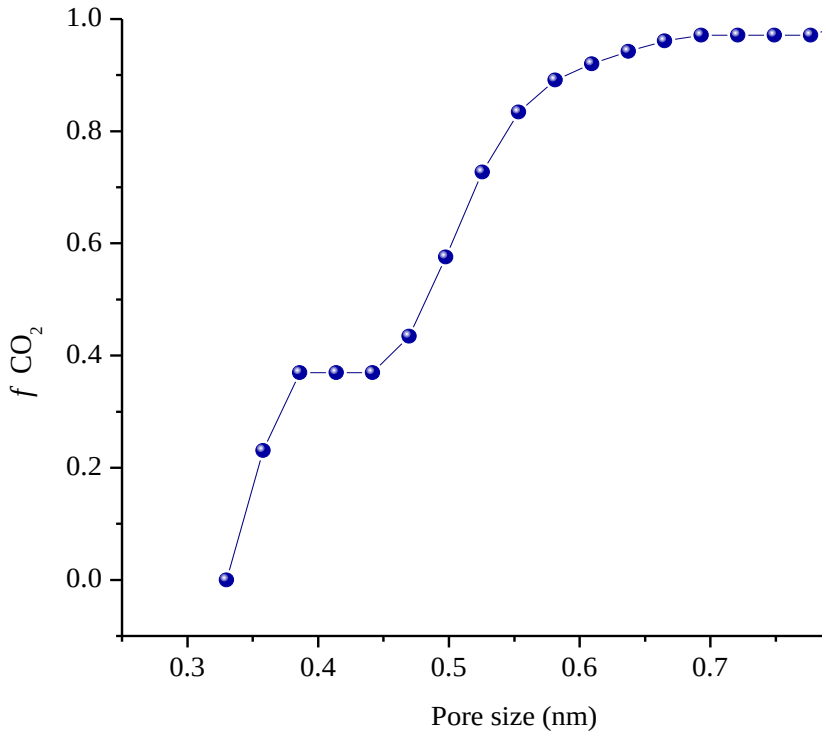

Fig. S8. Pore filled by CO_2 with average micropore size of sample IV-N deduced by applying the NLDFT model to CO_2 isotherms at 0 °C.

Tables

Table S1. Conditions used in the microwave pyrolysis experiments, yields and specific energy

Sample	Power (W)	Time (min)	Specific energy (kJ/g)	Bio-char yield (%)	Bio-oil yield (%)	Bio-gas yield* (%)
1-NS	300	3	4.1	18.0	23.7	58.3
II-NS	300	4	5.6	17.0	23.2	59.8
III-NS	300	5	7.5	16.8	37.0	46.2
IV-NS	300	6	8.0	17.5	39.0	43.5
V-NS	400	2	3.8	17.6	21.5	60.9
VI-NS	400	3	6.0	17.0	27.4	55.6
VII-NS	400	4	8.4	16.0	24.8	59.2

*Calculated by difference.

The specific absorbed energy (E) was determined by numerical integration of the absorbed power, (P_a), according to the following equation:

$$E = \frac{\int P_a dt}{M} \quad (1)$$

Where E is the specific absorbed energy (kJ g^{-1}), t is time differential (sec), and M is the initial mass of the sample (g).

The percent of absorbed and reflected power was calculated from the signals of incident and reflected power.

Table S2. Comparative CO_2 uptake capacities and preparation conditions of bio-chars

Precursor	**Conventional Temperature/ time (°C/ min)**	**Modification**	**Microwave power/time (W/min)**	**[a]CO_2 adsorption (mmol g^{-1})/T (°C)**	**S_{BET} (m^2 g^{-1})**	**V_{tot} (cm^3 g^{-1})**	**V_{micro} (cm^3 g^{-1})**	**Reference**
Nut shell	-	-	300/6	2.50/0	187	0.075	0.066	This work
Nut shell	-	-	300/6	2.0/25	187	0.075	0.066	This work
Rice straw	-	-	200/20	1.75/25	122	0.08	0.03	(Huang et al., 2015)
OP shell	-	KOH (2.5/1)	750/30	1.70/25	1069	0.52	0.42	(Hoseinzadeh Hesas et al., 2015)
Cane bagasse	600	-	-	1.67/25	388	-	-	(Creamer et al., 2014)
Walnut shell	900	-	-	1.65/25	397	0.198	0.159	(Lahijani et al., 2018)
Hickory wood	600	-	-	1.32/25	401	-	-	(Creamer et al., 2014)
Hickory chips	600	-	-	1.10/25	370	0.158	0.145	(Xu et al., 2019)
Sewage sludge	500/240	-	-	0.40/25	10	0.022	-	(Xu et al., 2016)
Pig manure	500/240	-	-	0.53/25	32	0.044	-	(Xu et al., 2016)
Wheat straw	500/240	-	-	0.78/25	20	0.041	-	(Xu et al., 2016)
Mesquite wood	850/120	-	-	1.92/25	126	0.07	0.03	(Dissanayake et al., 2020)
Mesquite chicke	850/120	-	-	1.60/25	255	0.15	0.10	(Dissanayake et al., 2020)
Soybean straw	900	CO_2-NH_3	-	1.86/30	764	-	-	(Zhang et al., 2016)

[a] Uptake at 1bar